Available online at www.sciencedirect.com
ScienceDirect
Optics Communications 275 (2007) 344–347
OPTICS COMMUNICATIONS
www.elsevier.com/locate/optcom

Temperature and strain discrimination using a single tilted fibre Bragg grating

Edmon Chehura, Stephen W. James, Ralph P. Tatam *

Engineering Photonics Group, School of Engineering, Cranfield University, Cranfield, Bedford MK43 0AL, UK

Received 19 January 2007; received in revised form 11 March 2007; accepted 16 March 2007

Abstract

A fibre optic sensor capable of discriminating between temperature and strain, using a single fibre Bragg grating, is presented. The technique exploits the core–cladding mode coupling of a tilted fibre Bragg grating (TFBG). The core and cladding modes exhibit different thermal sensivities, while the strain sensivities are approximately equal. Monitoring the core–core mode coupling resonance and the core–cladding mode coupling resonance of the TFBG spectrum allows the separation of the temperature and strain induced wavelength shifts.

Keywords: Temperature; Strain; Sensor; Tilted fibre Bragg grating; FBG; TFBG

The discrimination of the temperature and strain responses of fibre Bragg grating, FBG, sensors has been a consistent area of research over the past 10 years, with a large number of articles describing a wide range of techniques [1]. The majority of the reported approaches have relied on the use of two sensors with different sensivities to temperature and strain. This has been achieved in a number of ways. Appropriate packaging can ensure that one of the sensors is shielded from one of the measurands [2]. FBGs with inherently different sensitivities may be used, for example, FBGs with different centre wavelengths [3], FBGs written in fibres of different composition [4] or with different diameters [5], or FBGs fabricated under different conditions [6,7]. Alternatively, the measurement from an FBG may be combined with that of a different sensing technique, for example, measuring the fluorescence lifetime of ions in doped optical fibre [8] or stimulated Brillouin scattering [9].

Single FBG approaches have been reported. The use of the measurand induced wavelength shifts of the 1st and 2nd harmonics of the reflection from an FBG have been used to separate the temperature and strain responses of a single sensor element [10]. This technique, however, requires the use of optical sources and spectrometers operating in widely differing areas of the optical spectrum. In an extension of the technique used in [5], a single FBG may be written across a splice between fibres of different diameters [11], or between fibres of different composition [12]. In a similar vein, techniques based on etching or packaging sections of a single FBG have been reported [13]. The different thermal sensitivity of the orthogonally polarised reflections from an FBG fabricated in Hi–Bi fibre has also been exploited [14]. The techniques are summarised in Table 1a. In this paper the use of the properties of a single tilted fibre Bragg grating, TFBG, to facilitate the discrimination of temperature and strain is reported.

A standard FBG consists of a refractive index modulation in the core of an optical fibre that acts to couple the fundamental forward propagating mode to the contra-propagating core mode at a wavelength that satisfies the phase matching condition. The spectrum of such a device consists of a narrow wavelength passband in reflection while the transmission spectrum exhibits a notch at the wavelength of the passband. A TFBG consists of a refractive index modulation that is purposely blazed relative to

* Corresponding author. Tel.: +44 123 475 4630; fax: +44 12 345 1566.
E-mail address: r.p.tatam@cranfield.ac.uk (R.P. Tatam).

0030-4018/$ - see front matter © 2007 Elsevier B.V. All rights reserved.
doi:10.1016/j.optcom.2007.03.043

Table 1a
Sensor systems referenced in this paper

Reference number	Sensor system
This paper	Single TFBG
[3]	Two Co-located FBGs
[4]	Two FBGs in fibres of different dopants
[5]	Two FBGs in fibres of different diameters
[9]	FBG and Brillouin scattering
[10]	1st and 2nd harmonic FBGs
[11]	1st and 2nd order harmonic FBGs
[12]	FBG on a splice region of two different fibres with one fibre specially packaged
[13]	FBG on a splice region of two different fibres
[15]	Single FBG in Hi–Bi fibre

the fibre axis in order to enhance coupling between the forward-propagating core mode and the contra-propagating cladding modes (Fig. 1). The contra-propagating cladding modes attenuate rapidly and are therefore not observable in reflection but are observed as numerous resonances in the transmission spectrum of the TFBG.

The spectral response of the TFBG is governed by the phase matching condition (Eq. (1)):

$$\lambda_i = (n_{\text{eff}}^{\text{co}} + n_i^{\text{clad}}) \cdot \frac{\Lambda_{\text{B}}}{\cos\theta} \tag{1}$$

where λ_i, $n_{\text{eff}}^{\text{co}}$, n_i^{clad}, θ, and Λ_{B} are the ith cladding mode resonance wavelength, effective index of the core, effective index of the ith cladding mode, blaze angle and grating period, respectively.

The exact form of the transmission spectrum is highly dependent on the tilt angle employed [15]. The cladding mode resonance wavelengths will be sensitive to differential changes in the indices of the cladding and core modes, which have been exploited previously to demonstrate a refractometer [16]. For a small tilt angle, it is possible to produce a well defined single loss band that is blue shifted with respect to the main Bragg feature [17], as shown in Fig. 2.

It is known from the work carried out on another core–cladding mode coupler, the long period grating (LPG), that differences in the sensitivities of the effective indices of the core and cladding modes facilitate multi-parameter sensing using a single sensor element [18]. The composition and/or geometry of the fibre can be used to tailor the response of the core–cladding mode coupling wavelength to particular measurands.

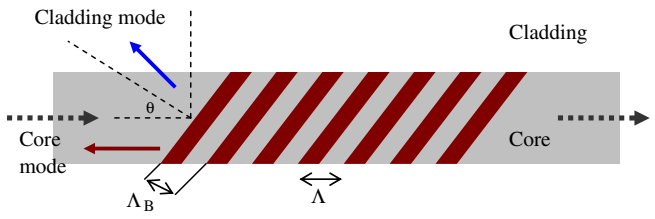

Fig. 1. Schematic diagram of a TFBG. Λ_{B}; grating peroid, Λ; grating period along the fibre axis, and θ; blaze angle. Dashed arrows represent the forward propagating core mode. Solid line represents coupling to cladding mode.

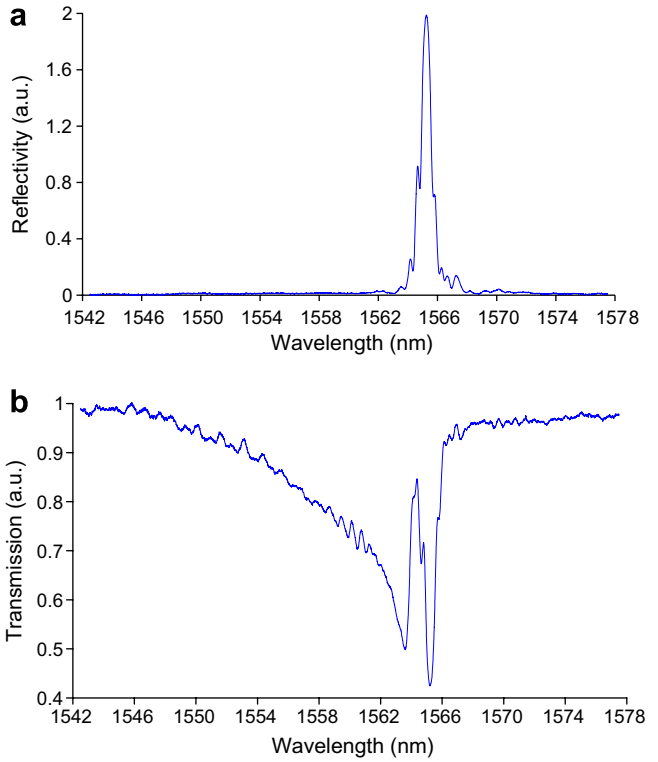

Fig. 2. (a) Reflection and (b) transmission spectra of a TFBG with tilt angle 1.5°, fabricated in hydrogen loaded boron–germanium co-doped optical fibre of cut off wavelength 1213 nm.

The TFBG spectrum contains a spectral feature corresponding to core–core mode coupling and features corresponding to core–cladding mode coupling. The technique presented here exploits the differences in the thermal and strain sensitivities of the core–cladding mode and core–core mode coupling resonances to facilitate simultaneous, independent measurement of strain and temperature using a single fibre grating.

A TFBG of length 5 mm, with blaze angle 1.5°, was fabricated in a boron–germanium co-doped optical fibre, Fibercore PS1250, with cut off wavelength of 1213 nm, using the near-field interference pattern of a tilted phase-mask. The photosensitivity of the fibre was enhanced by pressurizing it in hydrogen for a period of 2 weeks at a pressure of 150 bars at room temperature. The phase mask was illuminated with a UV beam at a wavelength of 244 nm and of average power 40 mW. The TFBG was interrogated by coupling the output from a super luminescent diode of bandwidth 60 nm into the optical fibre, and monitoring the transmission using a scanning fibre Fabry–Perot interferometer of free spectral range 43 nm and finesse 900 [19]. The reflection and transmission spectra are shown in Fig. 2.

One side of the TFBG was anchored to a fixed block, while the other was attached to a block mounted on a translation stage, via which a known extension and thus strain could be applied. The TFBG was enclosed within a

furnace that allowed the temperature to be controlled to within 1 K. The strain and temperature induced wavelength shifts of the core–core mode, Bragg, coupling and of the core–cladding mode coupling are plotted in Fig. 3. The linear fit to the data sets demonstrates that the system response can be described as linear. The contribution from any cross-sensitivity terms will not be significant over temperature ranges commonly encountered, for example, in structural monitoring [20,21]. The responses may therefore be expressed in terms of a matrix, Eq. (2), the inverse of which would be used to determine independently temperature and strain.

$$\begin{pmatrix} \Delta\lambda_{\text{core}} \\ \Delta\lambda_{\text{clad}} \end{pmatrix} = \begin{pmatrix} K_{\text{core},\varepsilon} & K_{\text{core},T} \\ K_{\text{clad},\varepsilon} & K_{\text{clad},T} \end{pmatrix} \begin{pmatrix} \varepsilon \\ T \end{pmatrix} \tag{2}$$

where $\Delta\lambda_{\text{core}}$ and $\Delta\lambda_{\text{clad}}$ are the wavelength shifts of the core–core mode resonance and of the core–cladding mode resonance respectively. From the results presented in Fig. 3, $K_{\text{core},\varepsilon} = 0.816 \pm 0.003$ pm/με, $K_{\text{clad},\varepsilon} = 0.830 \pm 0.03$ pm/με, $K_{\text{core},T} = 4.222 \pm 0.1$ pm/°C and $K_{\text{clad},T} = 6.021 \pm 0.07$ pm/°C are the sensitivity coefficients calculated for the core–core mode resonance (Bragg peak) and for the core–cladding mode resonance.

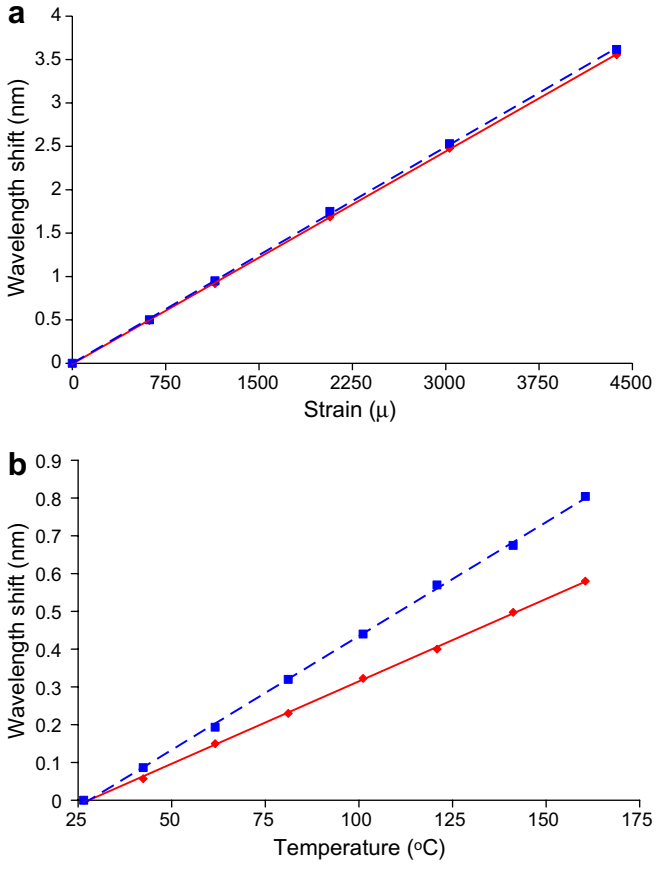

Fig. 3. (a) Strain and (b) temperature sensitivity of the resonance features of a TFBG with tilt angle 1.5°, fabricated in hydrogen loaded boron–germanium co-doped optical fibre of cut off wavelength 1213 nm. ◊ (red): core–core (Bragg) mode resonance and ■ (blue): core–cladding mode resonance. The lines are best fits to data points. (For interpretation of the references to colour in this figure legend, the reader is referred to the web version of this article.)

A common method of assessing the performance of a temperature–strain discrimination system is via the condition number of the matrix, which provides an indication of the sensitivity of the matrix operation to uncertainties in the matrix elements [22,23]. The errors that influence temperature–strain discrimination arise from the accuracy with which the system parameters that respond to temperature and strain are measured as well as errors arising from determining the components of the sensitivity matrix.

Table 1a describes the sensor systems that are referenced in this paper while the corresponding matrix inversion condition numbers are shown in Table 1b. The condition number of the approach reported in this paper is 39.4. This is comparable to that of the best performing single FBG approach, reported in [13], in which a single FBG was fabricated across a splice formed between two different fibre types, but with one fibre type bonded to a substrate of large thermal expansion coefficient. The smallest condition number, of 5.5, was determined for the system employing an FBG and stimulated Brillouin scattering [9], where the Bragg wavelength and Brillouin gain frequency have significantly different temperature and strain responses.

Table 1b also details the strain and temperature errors that were calculated using formulations reported in [23]. These errors depend on the wavelength measurement precision and on uncertainties in the determination of the matrix-element. In addition, the errors depend on the values of the applied strain and temperature [23]. Three types of strain and temperature errors are reported here; (i) maximum (accumulated) errors, where the errors arise only from the precision of the wavelength measurement, (ii) maximum (accumulated) errors where errors arise only from the uncertainties in the matrix-element values, and (iii) errors due to both the wavelength measurement precision and to the matrix element uncertainty (errors not calculated cumulatively). Errors obtained by taking the modulus of individual terms in the error-formulae are referred to as maximum or cumulative errors as they provide the worst possible error scenario. Non-cumulative errors are those obtained by taking into consideration the actual sign of the individual terms in the error-formulae and are therefore more representative than the maximum errors. A wavelength measurement resolution of 1 pm is assumed for all calculations. The temperature and strain were assumed to be 50 °C and 1000 με to allow the determination of the maximum error that might be experienced in a typical structural monitoring application. The matrix element uncertainties used in these calculations were the standard deviations that were reported in the references.

Table 1b shows that the matrix condition number is not sufficient on its own to describe the strain–temperature discrimination performance of a system. It can be seen that small condition numbers do not necessarily correlate with small strain and temperature errors. The condition number

Table 1b
A description of temperature–strain discrimination performances of the sensors listed in Table 1a (i) qualitatively by using condition numbers and (ii) quantitatively using mathematical formulations reported in [23]

Reference number	Error analysis according to [23]						Inversion matrix condition number
	λ-Measurement induced errors		Matrix-calculation induced errors		λ- and matrix-induced errors		
	ΔT (°C)	$\Delta\varepsilon$ ($\mu\varepsilon$)	ΔT (°C)	$\Delta\varepsilon$ ($\mu\varepsilon$)	ΔT (°C)	$\Delta\varepsilon$ ($\mu\varepsilon$)	
[9]	–	–	–	–	–	–	5.5
[12]	0.03	13	–	–	–	–	38.6
This paper	1	7	5	32	1	11	39.4
[13]	1	10	3	30	2	13	105.6
[3]	2	17	4	45	1	12	129.5
[5]	2	22	10	97	2	14	143
[4]	2	18	4	33	0.6	6	148.2
[11]	2	19	2	22	0.3	3	156.8
[10]	2	24	9	100	9	92	238.2
[15]	4	28	36	249	1	0.8	255.0

therefore only provides a qualitative analysis [23]. The condition number is calculated based on maximum errors in a measurement system [24] and for this reason the results of Table 1b shows some agreement between this number and the maximum/cumulative errors. The errors of ± 1 °C and ± 11 $\mu\varepsilon$ obtained from the TFBG sensor reported in this paper are comparable to errors of ± 1 °C and ± 12 $\mu\varepsilon$ calculated for a two co-located FBG sensor system [3] (two different wavelengths). However, the difference between the condition numbers of the two systems, 39.4 and 129.5, respectively, is significant.

In summary, a new approach to discriminating between the temperature and strain responses of FBG sensors has been demonstrated. The technique requires the use of a single FBG, tracking features that lie within the same spectral range, and does not require special processing or packaging of the fibre. The use of a small tilt angle that facilitates efficient coupling to a single cladding mode is beneficial, as its spectrum occupies a considerably narrower range than that occupied by TFBGs with larger tilt angles. Thus it allows wavelength division multiplexing to be employed. The main limitation of this approach lies in the fact that the system must be operated in transmission, which removes one of the benefits of FBG sensors – namely single ended operation.

Acknowledgement

The authors gratefully acknowledge the support of the Engineering and Physical Sciences Research Council (EPSRC), UK.

References

[1] O. Frazao, L.A. Ferreira, F.M. Araujo, J.L. Santos, Fibre Int. Opt. 24 (2005) 227.
[2] V.V. Spirin, M.G. Shlyagin, S.V. Miridonov, I. Marquez, Opt. Laser Technol. 33 (2001) 43.
[3] M.G. Xu, J.L. Archambault, L. Reekie, J.P. Dakin, Electron. Lett. 30 (1994) 1085.
[4] P.M. Cavaleiro, F.M. Araujo, L.A. Ferreira, J.L. Santos, F. Farahi, IEEE Photon. Technol. Lett. 11 (1999) 1635.
[5] S.W. James, M.L. Dockney, R.P. Tatam, Electron. Lett. 32 (1996) 1133.
[6] X.W. Shu, Y. Liu, D.H. Zhao, B. Gwandu, F. Floreani, L. Zhang, I. Bennion, Opt. Lett. 27 (2002) 701.
[7] X.W. Shu, D.H. Zhao, L. Zhang, I. Bennion, Appl. Opt. 43 (2004) 2006.
[8] S.A. Wade, D.I. Forsyth, Q. Guofu, X. Chen, T.S. Chuan, W. Yong, T. Sun, K.T.V. Grattan, Meas. Control 34 (2001) 175.
[9] M.A. Davis, A.D. Kersey, IEE Proc. – Optoelectron. 144 (1997) 151.
[10] G.P. Brady, K. Kalli, D.J. Webb, D.A. Jackson, L. Reekie, J.L. Archambault, IEE Proc. – Optoelectron. 144 (1997) 156.
[11] B.O. Guan, H.Y. Tam, H.L.W. Chan, C.L. Choy, M.S. Demokan, Microwave Opt. Technol. Lett. 33 (2002) 200.
[12] O. Frazao, J.L. Santos, J. Opt. A 6 (2004) 553.
[13] Z.Y. Zhao, S. Zhang, Y.S. Yu, Z.C. Zhuo, Y. Qian, Y.H. Cao, J. Zhang, W. Zheng, Y.S. Zhang, Microwave Opt. Technol. Lett. 43 (2004) 324.
[14] G.H. Chen, L.Y. Liu, H.Z. Jia, J.M. Yu, L. Xu, W.C. Wang, IEEE Photon. Tech. Lett. 16 (2004) 221.
[15] T. Erdogan, J.E. Sipe, J. Opt. Soc. Am. A 13 (1996) 296.
[16] G. Lafont, P. Ferdinand, Meas. Sci. Technol. 12 (2001) 765.
[17] S. Baek, Y. Jeong, B. Lee, Appl. Opt. 41 (2002) 631.
[18] S.W. James, R.P. Tatam, Meas. Sci. Technol. 14 (2003) R49.
[19] C.-C. Ye, S.E. Staines, S.W. James, R.P. Tatam, Meas. Sci. Technol. 13 (2002) 1446.
[20] G.M.H. Flockhart, R.R.J. Maier, J.S. Barton, W.N. MacPherson, J.D.C. Jones, K.E. Chisholm, L. Zhang, I. Bennion, I. Read, P.D. Foote, Appl. Opt. 43 (2004) 2744.
[21] M.J. O'Dwyer, C.-C. Ye, S.W. James, R.P. Tatam, Meas. Sci. Technol. 15 (2004) 1607.
[22] W. Jin, W.C. Michie, G. Thursby, M. Konstantaki, B. Culshaw, Opt. Eng. 36 (1997) 2272.
[23] W. Jin, W.C. Michie, G. Thursby, M. Konstantaki, B. Culshaw, Opt. Eng. 36 (1997) 598.
[24] A.M. Vengsarkar, W.C. Michie, L. Jankovic, B. Culshaw, R.O. Claus, J. Lightwave Technol. 12 (1994) 170.